Water Pipe Leak Detection Using Electromagnetic Wave Sensor for the Water Industry

J. H. Goh, A. Shaw, J.D. Cullen, A. I. Al-Shamma'a
Liverpool John Moores University, Built Environment and Sustainable Technologies (BEST) Research Institute, RF and Microwave Research Group, Henry Cotton Building, 15-21 Webster Street, Liverpool, L3 2ET, UK

M. Oliver, M. Vines, M. Brockhurst
Balfour Beatty Utility Solutions, West Service Road, Raynesway, Derby, DE21 7BG, UK

***Abstract*- This project concerns the use of an electromagnetic sensor for the detection of leaks/cracks in water pipes. As old metal pipes corrode, they start to become brittle, resulting in the potential for cracks to appear in the pipes. In addition corrosion can build up resulting in a restricted flow of water in the pipe. Using an electromagnetic (EM) sensor to monitor the signal reflected from the pipes in real time, provides the necessary information to determine where a leak in the pipe has occurred. Analysis of the reflected signal can provide the operator with information about the condition of the leak within the pipe. This work describes how the system was designed, and also its construction at a scale suitable for insertion into a 100mm diameter water pipe.**

I. Introduction

The purpose of this project is to reduce the water loss from public water supply distribution networks by identifying leaks in cast iron pipes. This research has investigated whether EM waves can be used to pinpoint the exact location of leaks in water pipes by using an internal EM wave sensor. This sensor is launched into the live drinking water mains through any existing hydrant and deployed using a mechanical drive on the launch chamber developed by Balfour Beatty [1]. The aim is to design a new sensor that can obtain a level of accuracy well above industrial demands.

The present technology used in the detection of leaks is acoustic and ground penetrating radar (GPR). Both of these techniques have their advantages and limitations. The acoustic [2,3] techniques are the most widely used in leak detection. They are based on the continuous analysis of the pipeline pressure, flow, temperature and density. The acoustic failed to perform optimally within the criteria of response time, robustness, reliability, sensitivity, accuracy and cost.

The GPR [4,5,6] uses low frequency EM waves to create an image of the subsurface by detecting the reflected signals from subsurface structures. It transmits the EM wave into the ground, and when the wave hits a buried object, the receiving antenna records a reflected signal. The GPR technique cannot differentiate between water, gas or oil pipelines and DSP [7] analysis required takes hours to complete. The water companies therefore still require a quick, cost justified, large scale method of identifying areas of actual leakage.

As a result, a new method was introduced which uses electromagnetic wave propagation.

II. Electromagnetic Theory For Leak Detection

Maxwell's equations [8] describe the relation of the electric and magnetic field to each other and to the position and motion of charged particles. Maxwell's equations relate the electric and magnetic fields to their sources, charge density and current density. The equations can be combined to show that light is an electromagnetic waves. The four fundamental electromagnetic equations are given in (1) to (4),

$$\nabla \cdot D = \rho \tag{1}$$

$$\nabla \cdot \mathrm{B} = 0 \tag{2}$$

$$\nabla \cdot \mathrm{E} = -\frac{\partial \mathrm{B}}{\partial t} \tag{3}$$

$$\nabla \cdot \mathrm{H} = J + \frac{\partial D}{\partial t} \tag{4}$$

In the above equations, E represents the electric field in volts per metre (Vm^{-1}) and H represents the magnetic field in amperes per metre (Am^{-1}). D is electric displacement field in coulombs per square metre (Cm^{-2}) and B is the magnetic flux density in tesla (T). J is the electric current density in amperes per square metre (Am^{-2}) and ρ is the electric charge density in coulombs per cubic metre (Cm^{-3}).

Water is transported in circular cross section metal pipes, which can be treated as a circular waveguide. Waveguide is a particular form of electrical transmission line that is generally used at microwave frequencies. When the pipe is filled with water, rather than air, it can operate at much lower frequencies, this is due to the speed of the EM wave in the two different mediums (water and air).

The speed of an EM wave in vacuum is approximately 3×10^8m/s, which is speed of light (c). The speed of an EM wave is reduced by a factor $\sqrt{\varepsilon_r \mu_r}$ when it travels through a material, where ε_r is the relative permittivity, and μ_r is the relative permeability of the material. ε_r for the water at the frequencies considered is approximately 81, at room temperature, and μ_r is 1, therefore, the speed of the EM wave

978-1-61284-691-0/11/$26.00 ©2011 IEEE

in fresh water at these frequencies is found approximately using equation 5,

$$c_{water} = \frac{c_{vacuum}}{\sqrt{\varepsilon_r \mu_r}} = \frac{3\times10^8}{\sqrt{81\times1}} = 3.33\times10^7\, m/s \qquad (5)$$

The electrical power is transported through a metal pipe by means of electromagnetic waves, which can take several different forms (modes), depending on the frequency the pipe dimensions and the material properties inside. This determines how the electric and magnetic fields appear in the pipeline.

The two most important modes in the circular waveguide are known as TE_{11} and the TM_{01} modes which are shown in Fig. 1. The solid line in Fig. 1 represents electric field and the dotted line represents the magnetic field. These modes differ from electromagnetic waves in free space because they have to be higher than a certain minimum frequency in order to be able to propagate through the pipe at all. For a typical 4 inch metal pipe, the so called cut off frequencies [9], below which there is no propagation is 192MHz for the TE_{11} mode and 251MHz for the TM_{01} mode. Consequently, between 192MHz and 251MHz, only the TE_{11} mode can propagate.

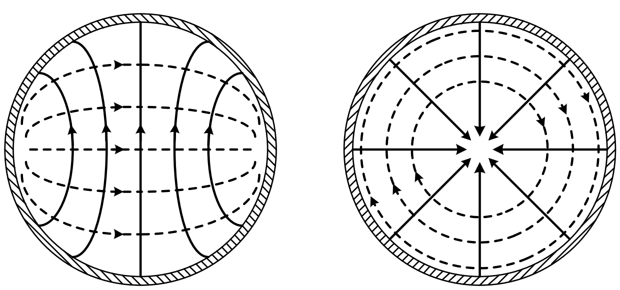

TE_{11} TM_{01}

Fig. 1. Electromagnetic mode patterns in a circular waveguide [10]

III. Loop Antenna

The loop antenna is a directional type antenna which consists of one or more complete turns of a conductor [11]. The loop antenna has a very low radiation resistance because it acts as an inductive component [12,13]. The advantages of the loop antenna is that it strongly responds to the magnetic field (H) of the EM waves, and is less affected by the man-made interference. The loop antenna also picks up less noise, providing a better signal to noise ratio (SNR).

IV. HFSS Simulation

High Frequency Structure Simulator (HFSS) [14,15] is a full wave electromagnetic wave simulator software which can be used to designed RF structures. The advantage of HFSS is that it allows complex geometries to be created compared to other packages. To determine the most suitable frequency range for the loop antenna, a simulation was run in HFSS. Fig. 2 shows the HFSS model of a 4 inch diameter cast iron cylinder filled with fresh water an antenna at each port.

To validate the HFSS simulations for the antenna, Fig. 3 shows the experimental setup for the water pipe. The water pipe was filled with water and two antennas were used. The length of the cast iron pipe was 510mm. A vector network analyzer (VNA) was used to sweep the frequency from 200MHz to 600MHz. The $|S_{11}|$ and $|S_{21}|$ results for the HFSS simulation and the experimental results are shown in Fig. 4 and Fig. 5.

In Fig. 4 both set of $|S_{11}|$ results have a similar underlying shape. The minimum of the both results is approximately at the same frequency region around 480MHz although the amplitude is different. Therefore, the reflection spectrum $|S_{11}|$ shows a level of agreement between the HFSS simulation and the experimental results, which shows that the operational frequency range determined by simulation is correct.

In Fig. 5 the shape of the both results is also comparable. The peak of the both results is clearly shown, but there is a slightly different in the resonant frequency with that of the experimental results being around 310MHz while the peak of the HFSS simulation is around 350MHz. This is likely to be due to the concrete liner on the inner surface of the cast iron pipe supplied by Balfour Beatty.

There is no clear resonance shape for the $|S_{21}|$, so it will be difficult to use to determine a leak. A resonant peak is clearly shown at around 480MHz for $|S_{11}|$, so this can be used to determine if there is a leak in the water pipe using the EM wave sensor system.

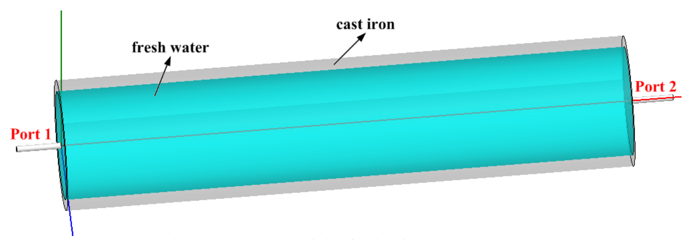

Fig. 2. HFSS model of 4 inch cast iron pipe

Fig. 3. Experimental of 4 inch cast iron pipe

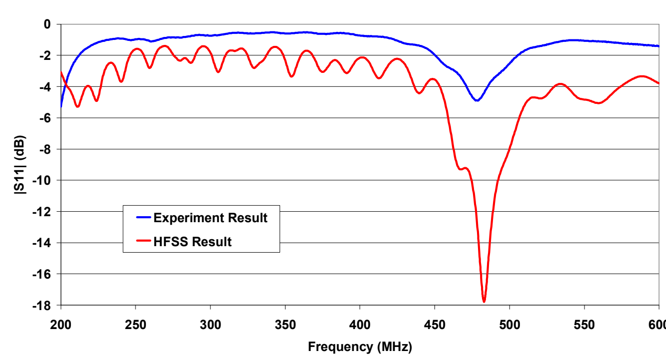

Fig. 4. Reflection signal $|S_{11}|$ of experiment and HFSS for loop antenna

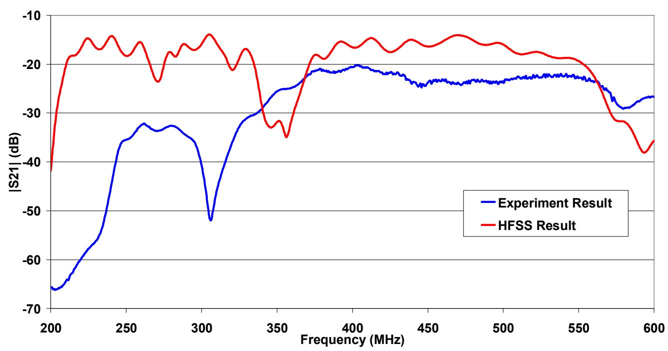

Fig. 5. Transmission signal $|S_{21}|$ of experiment and HFSS for loop antenna

It was then necessary to repeat the tests with a cracked pipe. A crack was made in the pipe and it was simulated using HFSS as shown in Fig. 6. The 4 inch cast iron cylinder is filled with fresh water and antennas at each port. A crack was made at the centre position on the cast iron cylinder. The simulation results for $|S_{21}|$ are shown in Fig. 7, and the attenuation caused for all crack widths, led to the signal dropping by 20dB. It can see the amplitude also falls as the width of the crack increases from 1mm to 10mm at 320MHz and 340MHz.

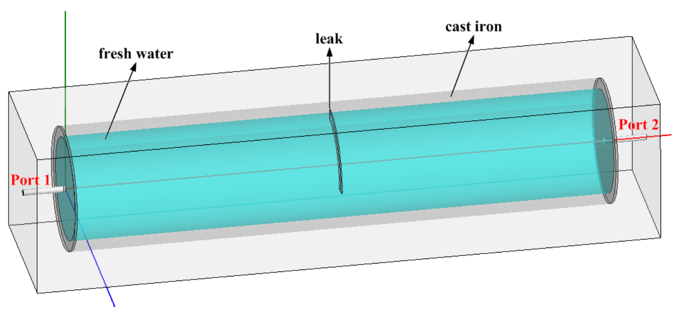

Fig. 6. HFSS simulation for water pipe leak

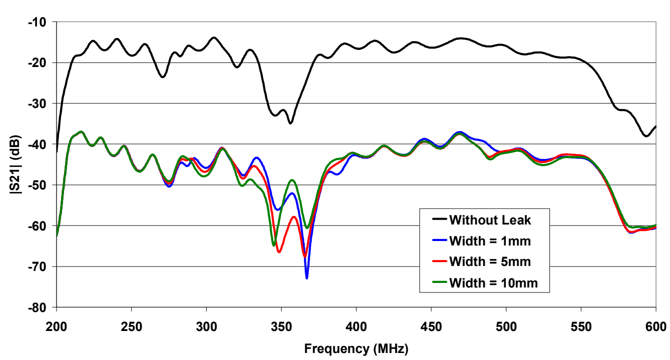

Fig. 7. Transmission signal $|S_{21}|$ of HFSS simulation result for water pipe leak

To validate the HFSS simulations for the water pipe leak, the experiment was setup as shown in Fig. 8. The pipe was totally filled with water and the two mild steel end caps were used to house an antenna at both ends. Then a 0.5mm crack was sawn in the central pipeline. The comparison results for this experiment with and without the crack are presented in Fig. 9. The attenuation at the lower frequencies the crack occurs on the signal for leakage pipe which same situation from the HFSS software simulation in previous simulation. The amplitude of the signals and the frequency of the resonance changes when the crack of the pipeline is made. The signal is down for 30dB at frequency region around 230MHz.

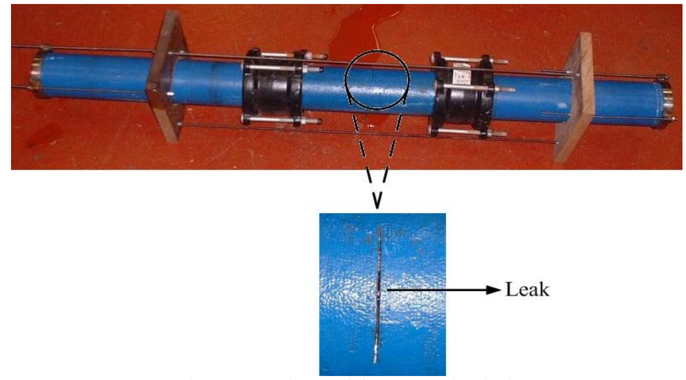

Fig. 8. Experimental for water pipe leak

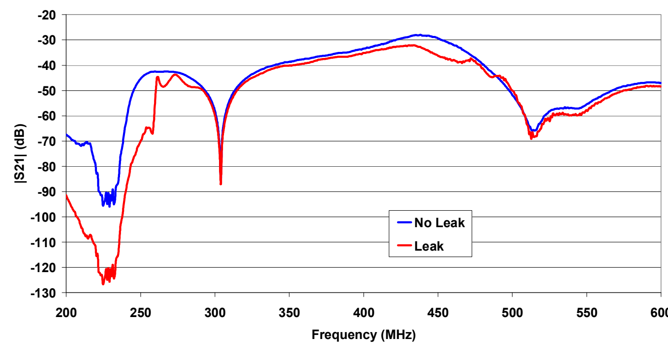

Fig. 9. Transmission signal $|S_{21}|$ versus frequency for water pipe leak

V. Prototype Sensor And Pcb Design

The next stage was to construct a sensor that could be moved inside the pipe. This consisted of a stainless steel body to house the electronics with a nylon spacer and a loop antenna at the front. The electronic housing allows the electromagnetic radiation to radiate efficiently from the antenna. The antenna is connected to the VNA via a coaxial feed cable.

The next step was to design a surface mount version of the electronics that could fit within the stainless steel housing. Fig. 10 shows the complete PCB circuit board fully populated with the components for the sensor. The components include the voltage controlled oscillator (VCO) ROS-535+, voltage regulator LM317, voltage amplifier CA3140E, directional coupler ADC-10-1R+ and power detector MAX2015.

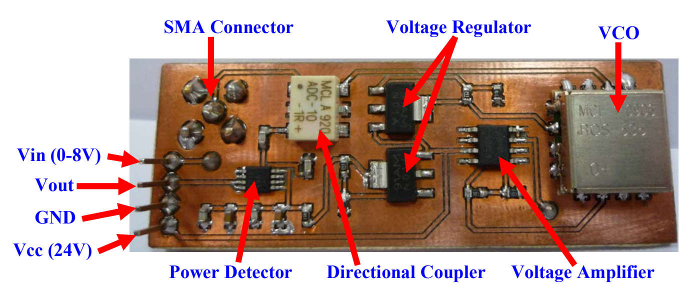

Fig. 10. Complete PCB circuit board with full components for the sensor

The PCB board was made using a computer numerical control (CNC) routing machine. The overall length of these circuit boards was 65mm and width was 22mm.

The block diagram for the electronics of a standalone EM wave sensor is shown in Fig. 11. For this circuit, a 24V power supply supplied the two voltage regulators (LM317) and the amplifier (CA3140E). The voltage regulators produced a 5V and 12V output voltages for the RF power detector MAX2015 and the voltage controlled oscillators (VCO) ROS-535+. LabVIEW programming software was used to control the NI Compaq DAQ with analogue output module NI9264 to produce an output voltage range from 0 to 8V, which was then amplified from 0 to 16V which will gives the full range of frequency output. The VCO produces a frequency sweep from 240MHz to 560MHz. The RF output from the VCO passes through a directional coupler ADC-10-1R+ and was then connecting to the antenna via an SMA connector. This allowed the reflected power to be measured via an RF power detector. The reflected signal power level is the $|S_{11}|$ parameter which is required for the RF signatures. The output from the RF power detectors is a DC voltage in the range of 0 to 2V which is then connected to the analogue input module NI9205 from which LabVIEW plots out the spectrum.

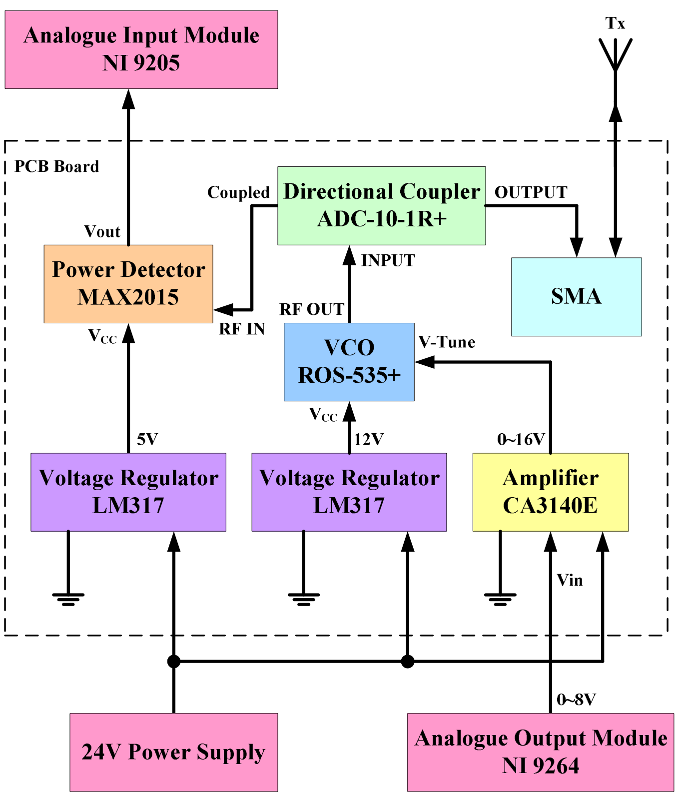

Fig. 11. Block diagram for PCB circuit board sensor

VI. Leak Detection

The final stage is to prove that the EM wave sensor can detect a leak in the pipeline. The first step is to obtain the reference signal spectrum for the 4 inch metal pipeline, then the sensor is put into the pipeline and the signal spectrum is compared with the reference signal. The signal comparison was done by the LabVIEW programme and the programme made a conclusion whether or not the pipeline needs further inspection.

Fig. 12 shows the experimental setup for leak detection. This experiment is setup with three 4 inch diameter pipelines sections connected together. These pipelines were mounted vertically and filled with water. The total length of the pipelines sections was 1480mm. The EM wave sensor with the electronics circuit which is shown in Fig. 10 was put into pipeline from the top of the pipe and the EM wave sensor passed through the centre of the pipeline.

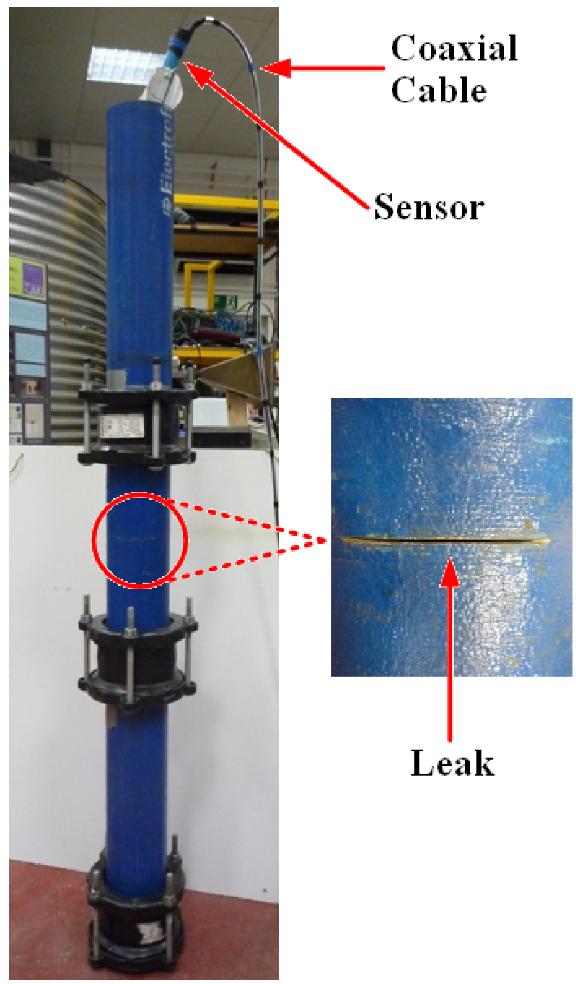

Fig. 12. Experimental setup for water pipe leak detection

The reference signal was taken at regular interval down the pipe and saved in a database. After that, a crack was made in the central pipeline to demonstrate that the EM wave sensor was able to detect leakage in the water pipeline. The crack was in the centre position of the second pipeline section away from any of the joints and at 74cm from top of the pipeline.

The measurements for the reflection signal $|S_{11}|$ were taken using the LabVIEW programme, and the reflection signal $|S_{11}|$ was compared with the reference signals that were obtained in the previous measurement. The LabVIEW programme then made a conclusion on whether the pipeline needed further inspection. Fig. 13 shows the waveform comparison for the signal at 70cm depth in the pipeline. The waveforms were then compared using the Pearson correlation statistic method via the LabVIEW programme. The resonance peak has a huge change and attenuation occurs for the signal spectrum at 70cm depth compared to the reference signals. The LabVIEW programme shows the 'Pipe Needs Visual Inspection' in Fig. 13, which mean that a leak has been detected at this region of the pipeline and needs further inspection.

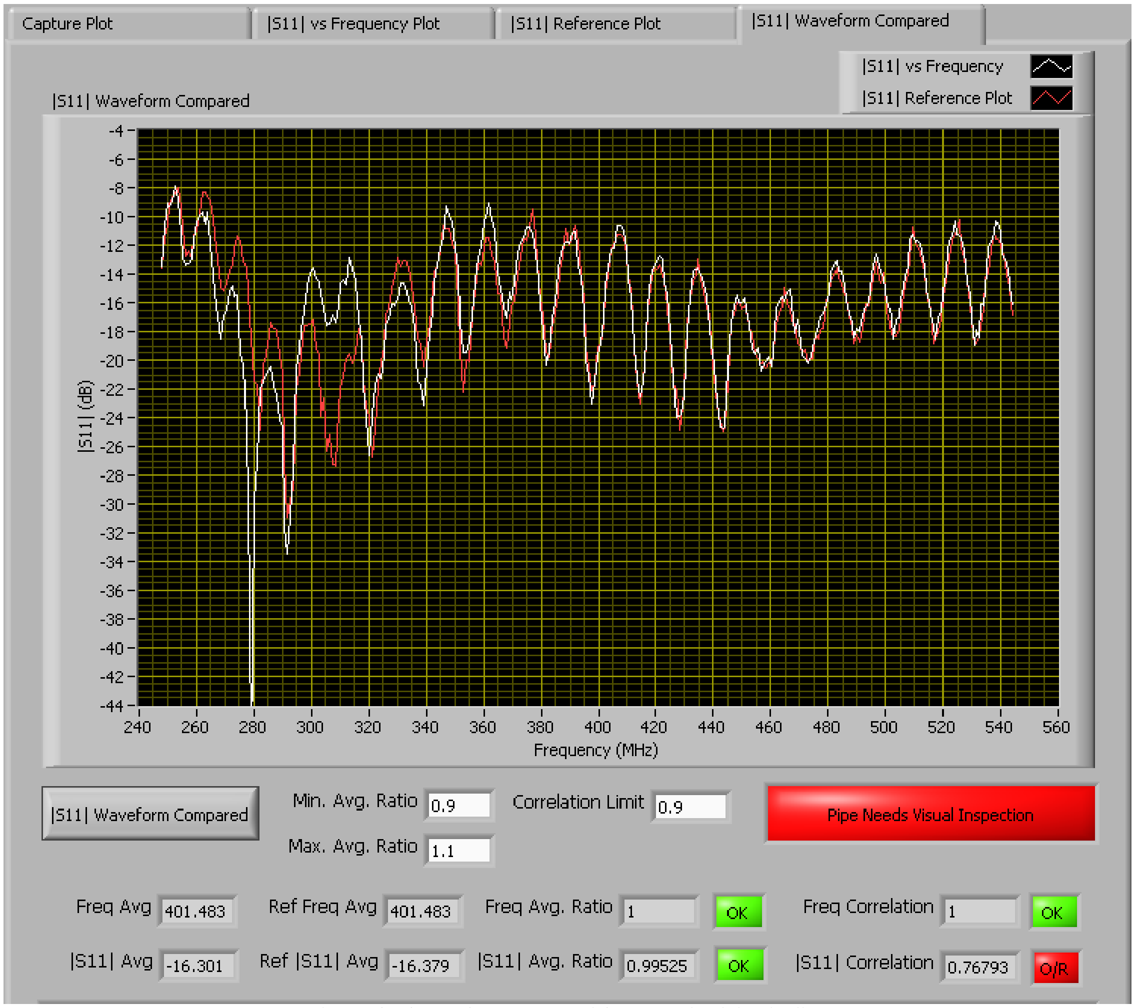

Fig. 13. $|S_{11}|$ waveform compared for 70cm depth in pipeline

VII. Conclusion

This research has proved that EM waves at high frequency in water are possible. Propagation of EM waves in water is affected by parameters including permittivity (ε) and conductivity (σ). The HFSS and experimental results showed good agreement throughout the project, and this helped in understanding the interaction between the water pipeline and the EM wave from the antenna. The attenuation was observed to be a good indication of water pipe leaks. The LabVIEW programme created for this project evaluates the output of the EM wave sensors and gives a recommendation about whether the water pipeline needs further investigation. For further work and development, leaks at different positions and the pipes with more than one leak should be investigated. Further work should also be done to improve the matching of the antenna to 50Ω which should improve signal strength.

References

[1] Balfour Beatty Utility Solutions, West Service Road, Raynesway, Derby, DE21 7BG, UK.

[2] D. B. Sharp and D. M. Campbell, "Leak Detection in Pipes Using Acoustic Pulse Reflectometry", Department of Physics and Astronomy, University of Edinburgh.

[3] M. J. Brennan, P. F. Joseph, J. M. Muggleton and Y. Gao, "Some Recent Research on the use of Acoustic Methods to Detect Water Leaks in Buried Plastic water Pipes", Institute of Sound and Vibration Research, University of Southampton.

[4] Mansor Nakhkash and Mohammad R. Mahmood-Zadeh, "Water Leak Detection Using Ground Penetrating Radar", IEEE Tenth International Conference on Ground Penetrating Radar, 21-24 June, 2004, pp. 525-528.
[5] Seung-Yeup Hyun, Yu-Sun Jo, Heon-Cheol Oh and Se-Yun Kim, "An Experimental Study on a Ground Penetrating Radar for Detecting Water-Leaks in Buried Water Transfer Pipes", IEEE Antennas, Propagation and EM Theory, 2003, pp. 597-599.
[6] S.R. Pennock, M.A. Redfern, and Q. Shan, "Subsurface Illumination And Propagation In Ground Penetrating Radar", Department of Electronic & Electric Engineering, University of Bath, IEEE Antennas and Propagation, 2006, pp. 1-5.
[7] Yumei Wen, Ping Li, Jin Yang and Zhangmin Zhou, "Information Processing in Buried Pipeline Leak Detection System", College of Opto-electronic Engineering, University of Chongqing , IEEE Information Acquisition, 2004, pp. 489-493.
[8] Joseph F. White, "High Frequency Techniques: An Introduction to RF and Microwave Engineering", A John Wiley & Sons, Inc, 2004
[9] David M. Pozar, "Microwave Engineering, 2nd Edition", John Wiley & Sons, Inc, 1998.
[10] John D. Kraus, "Electromagnetics, 4th Edition", McGraw-Hill International Editions, 1992.
[11] K.F. Lee, "Principles of Antenna Theory", Wiley, 1984.
[12] Joseph Carr, "Antenna Toolkit, 2nd Edition", Newnes, 2001.
[13] John D. Kraus and Ronald J. Marhefka, "Antennas For All Applications, 3rd Edition", McGraw-Hill International Editions, 2002.
[14] Ansoft Corporation, "Parametrics and Optimization using Ansoft HFSS", Product Feature, Horizon House Publications, 1999.
[15] D. M. Park and J. J. Choi, "Three-Dimensional Simulation of X-Band Coupled Cavity Traveling Wave Tube Amplifier", Journal of the Korean Physical Society, Vol.43, No. 6, Dec 2003, pp.1150-1111.